Strong Conductance Variation in Conformationally Constrained Oligosilane Tunnel Junctions†

Christopher B. George,* Mark A. Ratner, and Joseph B. Lambert

Department of Chemistry, Northwestern University, Evanston, Illinois 60208

Received: November 12, 2008

The effects of molecular conformation on conductance in oligosilane-bridged metal−molecule−metal junctions are studied theoretically using density functional theory combined with a nonequilibrium Green's function approach. Varying the internal SiSiSiSi dihedral angles in hexasilane diamine chains changes the conductance by up to 3 orders of magnitude. This conformational dependence is due to the effects of σ-delocalization on the positions of the highest occupied molecular orbital (HOMO) energies. The conductance values for the different conformations are related to electron transfer rates in donor−bridge−acceptor systems, and the effect of shifting the injection energy is examined. The transport properties are found to be extremely sensitive to the alignment between the HOMO energies and Fermi level of the gold electrodes.

I. Introduction

Development of molecular electronic devices requires careful tailoring of the electronic transport properties to achieve the desired functionalities.[1,2] One approach for engineering specific transport properties that has been studied theoretically[3−6] and realized experimentally[7,8] controls the effect of molecular conformation on conductance. Recent experiments[7] have shown that extending π-conjugation to varying degrees in a biphenyl system by altering the twist angle between the two phenyl rings affects the electronic transport, with a conformational dependence predicted by π-orbital overlap arguments.[3,4,9]

The conformational dependence of the electronic properties of π-conjugated molecules has an analogue in the electronic properties of σ-conjugated molecules. Methylated and catenated oligosilanes have been the subject of research studying the effects of σ-delocalization on optical properties such as UV and IR absorption.[10−20] These studies indicate that σ-delocalization is extended by *anti* turns (SiSiSiSi dihedral angles of 180°) but not by *cisoid* turns (small dihedral angles) in the backbone of silane chains. Given the phenomenon of conformation-dependent transport in π-conjugated structures, it is worth examining whether σ-conjugated structures exhibit a similar effect.

In this work, we examine theoretically how the conformational dependence of the electronic properties of oligosilane chains can be used to control electronic transport in single molecule junctions. Charge transport properties are calculated for a series of amine-terminated hexasilane chains between gold electrodes with varying internal dihedral angles ranging from 0° to 180° (Figure 1). Zero-bias conductances for the chains are computed by using a combination of density functional theory (DFT) and nonequilibrium Green's function (NEGF) techniques.[21] The results indicate a strong dependence of the conductance on the silane backbone conformation and are understood by using an analysis of the offsets between the highest occupied molecular orbital (HOMO) energies and the Fermi level for the different conformations. Comparisons with results from the Hückel-type Ladder C model[16,18] confirm the role of σ-delocalization in the transport properties.

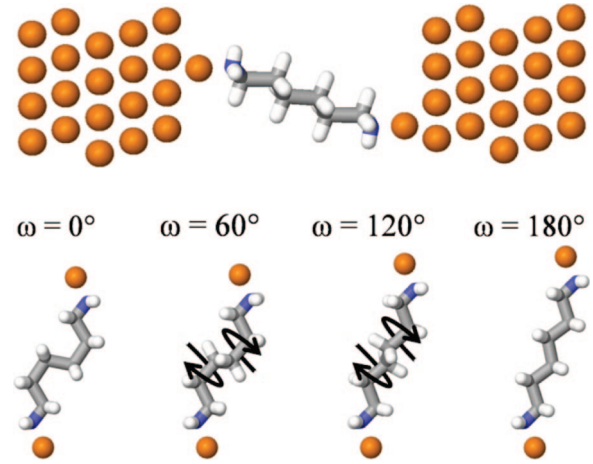

Figure 1. Model of an $NH_2-(SiH_2)_6-NH_2$ molecule between extended gold electrodes modeled by single adatoms above 4×4 Au[111] layers. The blue atoms are nitrogen, gray atoms are silicon, white atoms are hydrogen, and gold atoms are gold. Below, four of the ten conformations studied are shown. The black arrows indicate the direction the dihedral angle has changed from the conformation to the left. Of the three silane dihedral angles in hexasilane diamine, the center angle remains ∼180° in all the structures while the outer angles change.

II. Computational Methods

Electronic transport properties are calculated for $NH_2-Si_6H_{12}-NH_2$ molecules sandwiched between gold electrodes in which the amine groups bond to coordinatively unsaturated gold adatoms[22,23] above 4×4 Au[111] slabs (Figure 1). The gold−amine bonding distance is determined by relaxing an $Au_{20}-NH_2-Si_6H_{12}-NH_2-Au_{20}$ system in which the amine groups are bonded to single gold apex atoms, as described in previous work.[24] This Au−N distance is fixed for the other silane conformations. The additional conformations with varying internal dihedral angles are generated by using DFT-based geometry relaxations in Q-Chem 3.0.[25] $Au-NH_2-Si_6H_{12}-NH_2-Au$ complexes undergo constrained relaxations in which

† Part of the "George C. Schatz Festschrift".

* To whom correspondence should be addressed. E-mail: (C.B.G.) c-george@northwestern.edu; (M.A.R.) ratner@chem.northwestern.edu; (J.B.L.) jlambert@northwestern.edu.

10.1021/jp809963r CCC: $40.75
Published on Web 03/12/2009

the Au−N bond distances are fixed at 2.33 Å, the two outer silane backbone dihedral angles are fixed at varying angles, and the Au−N−N−Au dihedral angle is fixed at 180°. The relaxations are performed by using the B3LYP hybrid exchange/correlation functional[26,27] with a 6-31g** basis set for the lighter atoms and the LANL2DZ effective core potential (ECP) for the gold atoms.[28] The complexes are then inserted between larger gold electrodes where each electrode consists of two 4×4 Au[111] layers. The gold adatoms are positioned in the hcp hollow sites with surface atom to adatom distances of 2.8 Å.[23]

Electronic currents are calculated from these geometries by using a NEGF/DFT formalism implemented in ATK 2.0.[29] Periodic DFT calculations are performed to calculate the electronic structure of the system, using the local density approximation (LDA) parametrized by Perdew and Zunger.[30] A single-ζ plus polarization basis set is used for gold atoms, and a double-ζ plus polarization basis set is used for all other atoms.

The zero-bias, low-temperature conductance is calculated by using

$$g = g(E_F) = \frac{e^2}{\pi\hbar} T(E_F) \quad (1)$$

where g is the conductance, T is the transmission, and E_F is the Fermi level. The zero-bias conductance can be related to the electron transfer (ET) rate in a donor−bridge−acceptor (DBA) system via the rough approximation[31]

$$g \approx \frac{8e^2}{\pi^2 \Gamma_D^{(L)} \Gamma_A^{(R)} F} k_{D\to A} \quad (2)$$

The $\Gamma_{(D,A)}^{(L,R)}$ parameters represent the broadening of the donor and acceptor levels due to their binding to the metallic electrodes, F is the thermally averaged Franck−Condon weighted density of nuclear states, and $k_{D\to A}$ is the electron transfer rate. Equation 2 is valid under the approximation that the donor and acceptor energies shift toward the Fermi level such that $E_D, E_A \cong E_F$, and the electronic structure of the bridging molecule remains relatively unchanged in the presence of the metallic electrodes. In the electron transport formalism, the donor and acceptor groups function as linkers from the bridge to the electrodes and the Fermi energy takes the place of the donor energy in the ET rate expression. By plotting the transmission as a function of energy, one can see how the zero bias conductance varies with injection energy, and consequently one can approximate how electron transfer rates vary with the donor energy; higher transmission values correspond to higher ET rates.

From eqs 1 and 2, it is clear that to obtain correct conductance and electron transfer values, an accurate calculation of $T(E_F)$is required. This value is strongly dependent on the offset between the HOMO energy level and Fermi level[32] for systems where hole transport dominates. If the Fermi energy lies far from the HOMO energy, the system will have a lower transmission than if the Fermi energy lies close to the HOMO. However, the use of DFT to describe the HOMO-Fermi level alignment has been shown to yield incorrect transport properties due to errors in the description of charge transfer between the molecule and electrode.[33−42] While remaining mindful of this potential source of error, we use the HOMO-Fermi level offset for hexasilane diamine between gold electrodes calculated in a previous study.[24] In that work, the HOMO energy of $Au_{20}-NH_2-Si_6H_{12}-NH_2-Au_{20}$ was approximated by its Kohn−Sham eigenvalue calculated by using DFT, and the band alignment was determined by finding the difference between the HOMO energy and the work function of gold (−5.1 eV).[43]

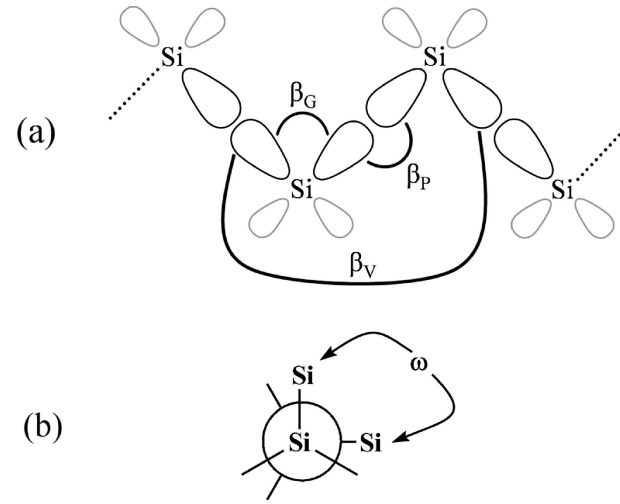

Figure 2. (a) Resonance integrals and (b) dihedral angle ω used in the Ladder C Hückel calculations. The geminal and primary interactions, denoted by β_G and β_P, remain unchanged as the dihedral angle ω of the silane backbone changes while the vicinal interaction, β_V, has a cosine dependence on the dihedral angle.

The role of σ-delocalization in determining the relative location of the HOMOs for peralkylated silane chains with different conformations can be understood with the Ladder C model,[16,18] a modified version of the Sandorfy C model.[44] The Hückel-type Ladder C model includes three types of resonance integrals (Figure 2) and a Coulomb integral α_{Si} to describe the electronegativity of the silicon sp^3 hybrid orbital. The β_G and β_P resonance integrals describe the geminal and primary interactions between sp^3 orbitals, respectively; they remain constant regardless of conformation. The β_V resonance integral has a $\cos(\omega)$ dependence on the dihedral angle ω (Figure 2), and is the only angle-dependent term. The values for these parameters, $\beta_G = -1.1$, $\beta_P = -3.5$, $\beta_V = 0.11 - 0.70\cos(\omega)$ (all values in eV), are obtained from a study by Schepers et al.[19] in which the integral values were optimized to best fit Hückel orbital energies to Hartree−Fock ab initio orbital energies for a range of different permethylated oligosilane conformers. By using dihedral angles from the same silane geometries as in the transport calculations, the Ladder C model is used to calculate HOMO energies for the different conformations to show what effect σ-delocalization has on the location of the HOMOs.

III. Results and Discussion

The transmission curves calculated with ATK for the different silane conformations are plotted in Figure 3. The position of the Fermi level is set by using the previously calculated HOMO-Fermi level offset of 0.27 eV[24] with the HOMO energy of the *all-trans* case used for the Fermi level alignment. The peaks near 1 eV are likely due to metal-induced gap states (MIGS).[45] The close proximity of the Fermi level to the HOMO energies results in the zero-bias conductance values (Figure 4) being highly sensitive to shifts in the relative HOMO energies within the series of different conformations. These shifts in HOMO energies are partly the result of σ-delocalization.

The addition of the β_G and β_V resonance integrals (Figure 2) as perturbative terms to the α_{Si} and β_P terms from the Sandorfy C model allows for a description of σ-delocalization within oligosilane systems.[46] As the dihedral angle ω increases from

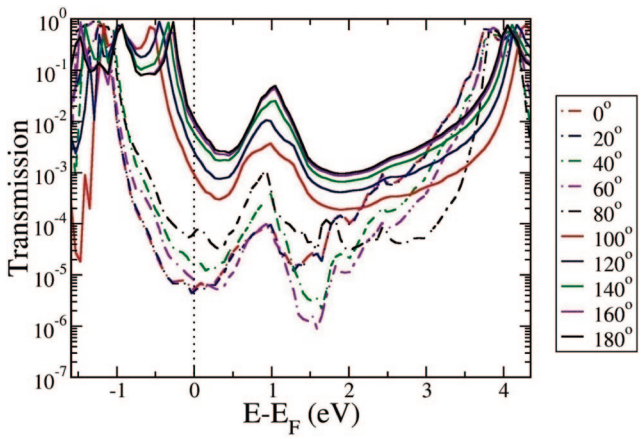

Figure 3. Transmission versus energy shifted from the Fermi energy for the different conformers, calculated using NEGF/DFT.[29] The dotted line corresponds to the Fermi energy. The peaks near 1 eV correspond to metal-induced gap states while the HOMOs lie just below the Fermi energy.

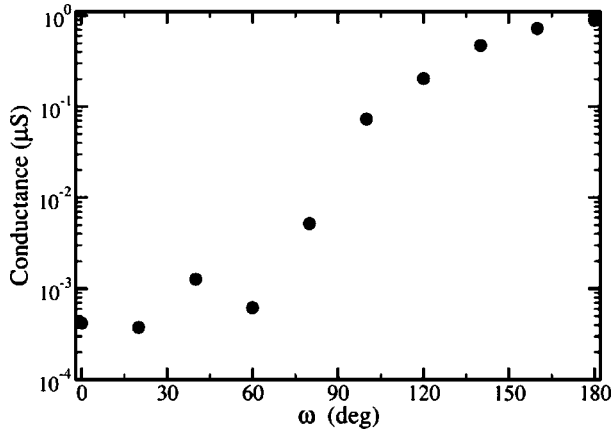

Figure 4. Conductance versus internal silane dihedral angles, ω. The range over several orders of magnitude is dependent upon the exact HOMO-Fermi level offset (calculations done with ATK 2.0).

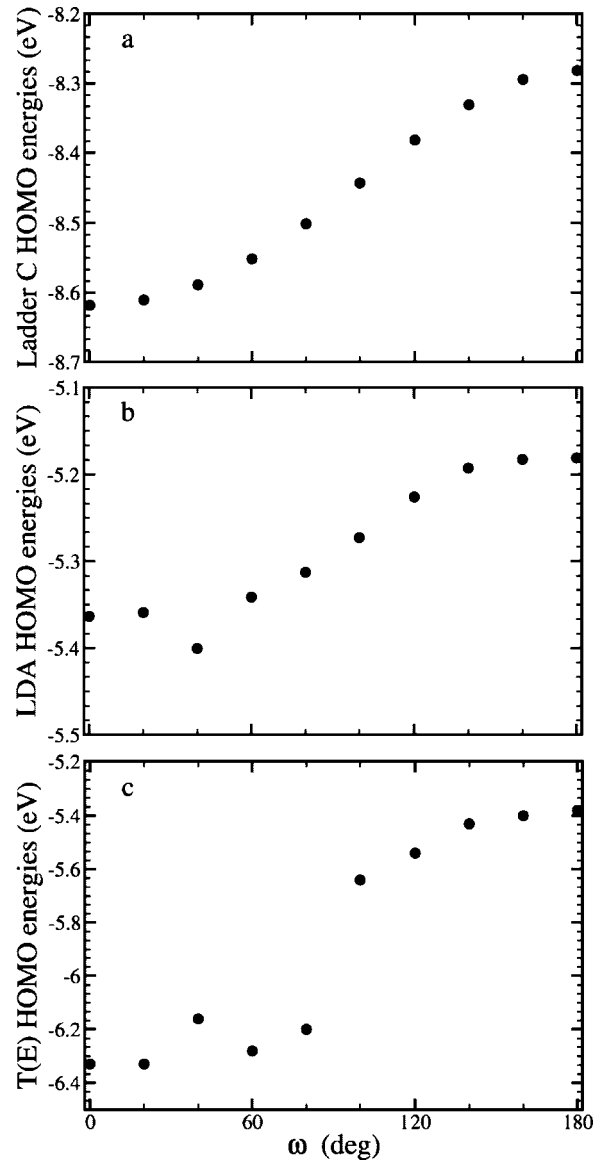

Figure 5. Highest occupied molecular orbital (HOMO) energies versus internal silane dihedral angles. The energies in part a are calculated by using the Hückel Ladder C model with parameters optimized to match ab initio results[19] for a methylated hexasilane chain. The energies in part b are computed by using DFT with the local density approximation (LDA) for hexasilane diamine. The results in part c are calculated by determining the location of the HOMO peaks in the transmission $T(E)$ plots. Absolute energies are obtained in part c by approximating the Fermi energy to be the work function of gold (−5.1 eV).[43]

0° to 180°, the value of β_V goes from negative to positive, and σ-delocalization increases as the interference between β_G and β_V goes from destructive to constructive.[19] At $\omega = 180°$, the HOMO is most destabilized due to the large, positive β_V term. Ladder C calculations of the different conformations' HOMOs (Figure 5a) exhibit the expected sinusoidal behavior, and HOMO energies calculated for hexasilane diamine conformations (without electrodes present) using DFT with the Perdew and Zunger parametrization[30] of the LDA (Figure 5b) exhibit a similar trend, albeit with a slightly different range of energies and an aberration at $\omega = 40°$. The disparities between the DFT and Ladder C results may be attributed to the different end groups on the silane chains in the two studies. In the DFT calculations, the silane chains are terminated by NH_2 groups while in the Ladder C calculations, the chains have $Si(CH_3)_3$ end groups. Also, the Ladder C parameters presented by Schepers[19] were suggested to describe methylated silane chains. The DFT calculations were performed on silane chains without methyl side groups.

The energies of peaks in the transmission plots corresponding to the conformations' HOMOs display the effects of σ-delocalization as well (Figure 5c). The presence of the gold electrodes causes the additional shifts in relative energies between the conformations as compared to the HOMO energies computed with DFT for the molecules without gold atoms. It is assumed that the HOMO of the molecule in the junction is still composed of the delocalized σ-bonding orbital that constitutes the HOMO of the isolated molecule. It has been shown[47] that aryl substitution in polysilane chains can lead to the HOMO having more π-like character, but the gold electrodes are not expected to have a similar effect.

The additional shifts observed in the HOMO energies for calculations in the junction (the energies of HOMO peaks in Figure 3) can be explained in part by the Au−N−Si bond angles for the different molecular configurations (Figure 6). Previous work by Hybertsen et al. has shown that the orientation of the amine end group with respect to the gold adatom it binds to affects the transport properties of alkyl diamine systems due to the directionality of the nitrogen's lone pair.[48] The Au−N−Si bond angles suggest that this effect works synergistically with σ-delocalization to increase the relative HOMO shifts and

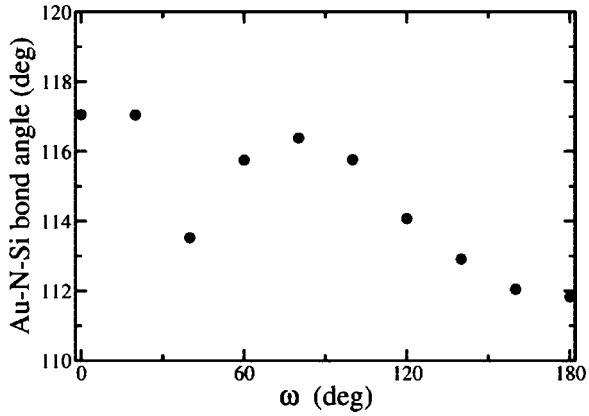

Figure 6. The bond angles of Au−N−Si versus silane dihedral angles. The small changes in Au−N−Si bond angles could contribute weakly to the more dominant effect that σ-delocalization has on the relative shifts in HOMO energies seen in transmission plots.

ultimately alter the conductance properties. Given the small changes in Au−N−Si bond angles, however, the dominant cause of the HOMO shifts is expected to be due to σ-delocalization.

Comparing the conductance results with the HOMO energies from the transmission plots in Figure 3 reveals the dramatic effect that σ-delocalization has on the transport properties of silane-bridged molecular junctions. The zero-bias conductance values follow the HOMO energies very closely leading to a variation of several orders of magnitude depending on the internal dihedral angles in the hexasilane backbone. Electron transfer rates in DBA systems with oligosilane bridges are expected to exhibit a similar conformational dependence, albeit with a smaller variation. Because the shifts in HOMO energies in the molecular junctions are partly due to the presence of the gold electrodes (Figure 5), the shifts in HOMO energies for oligosilanes in DBA systems will likely be smaller and therefore cause less variation in the ET rates. However, the general trends calculated for the conductance values are expected to hold for DBA systems in which the donor energy lies close to the HOMO energy of the bridging molecule.

The conformational dependence of the zero-bias conductance values is highly sensitive on the band alignment between the HOMOs and Fermi level, as seen from the spectral representation of the conductance[31] and Figure 3. If the Fermi level is close to the HOMOs, the trend in conductance values follows the trend in orbital energies predicted by the Ladder C model. If the HOMO-Fermi level offset is larger (greater than ∼1.5 eV), that trend begins to break down. Recent experimental results[49] from photoinduced electron transfer reactions with conformationally constrained tetrasilane bridges can be understood by using such an analysis.

Shibano et al.[49] report that charge recombination rates in DBA systems with permethylated silane bridging molecules exhibit very little conformational dependence, and that charge recombination rates are actually lowest for unconstrained silanes compared to constrained silanes with $\omega = 0°$ or 180°. This is contrary to our conductance results which indicate that the $\omega = 0°$ conformation should have the lowest recombination rate. This disparity can be understood by examining the energy region beyond 1.25 eV in the transmission (Figure 3) and recalling the close relation between transmission and ET rates presented in eqs 1 and 2. If the electron injection energy is greater than the *all-trans* bridging silanes' HOMO by over ∼1.5 eV, then the zero-bias conductance results for the $\omega = 0°$ conformation would no longer be lowest; the conductance, and consequently ET rate, for the $\omega = 60°$ or 80° conformation would be lowest. Given the low barrier for conformational changes in oligosilanes,[11] it is likely that the unconstrained silane would sample the $\omega = 60°$ and 80° conformations leading to a lower average conductance than the $\omega = 0°$ case. At injection energies near the bridging silanes' HOMO energies, conductance results and experimental electron transfer results are expected to agree. Additionally, if an electronic resonance is approached, the Landauer-based eq 1 needs[2] to be corrected by vibronic effects.

IV. Conclusion

Electronic transport properties of hexasilane diamines bridging gold electrodes to form metal−molecule−metal junctions have been computed. The effects of σ-delocalization on the junctions' zero-bias conductance values have been studied by using a series of hexasilanes with different dihedral angles in the silane backbones. The results indicate that a strong conformational dependence exists in the conductance values due to the shifting of HOMO energies in the transmission, with predicted conductance values spanning several orders of magnitude. The HOMO energy shifts can be explained by changes in the σ-delocalization of the silane chains, and the σ-delocalization can be understood by using the Hückel-type Ladder C model.[16,18]

Previously, it was shown that the decay in conductance with increasing length in silane-bridged molecular junctions is less steep than the decay in alkane-bridged junctions.[24] However, the exact value of the decay constant in the silane-bridged systems is extremely sensitive to the HOMO-Fermi level alignment. The same sensitivity exists for the conformational dependence of the conductance. For HOMO-Fermi level offsets less than ∼1.5 eV, the trend in conductance values for the different conformations follows the trend in HOMO energies. For larger offsets, the similarity between the shifts in relative HOMO energies and conductance values begins to fade. This is likely due to the actual form of the Green's functions that enter the transmission T in eq 1 quadratically.[21] For orbital energies close to the Fermi energy, the transmission is dominated by the closest accessible orbital. As the gap increases, many orbitals make comparable contributions, so the simple correlation of the conductance with the HOMO-Fermi level offset is expected to fail. The existence of two regimes in the transmission is a potential explanation for why experimental electron transfer results in constrained tetrasilane chains may differ from the ET rates expected from our conductance results.

One of the major potential benefits of molecular electronics is the additional control over electronic current that is not present in traditional semiconductor junctions. By changing the shape of the molecular "wire" in silane-bridged metal−molecule−metal junctions, the (small injection gap) electronic transport properties can be modified very substantially. Exploiting the properties of σ-delocalization in silane chains introduces an additional dimension to transport in σ-bonded molecules that could lead to an increased functionality of silane-based molecular wires in nanoscale electronics.

Acknowledgment. This work has been partially supported by the NSF division of Chemistry and the NSF Materials division through the Northwestern MRSEC. The NSF-NNI is thanked for their support, through the Purdue Nanohub. C.B.G. is supported by a Graduate Research Fellowship from the NSF. The authors thank Gemma Solomon, James Greer, and Josef Michl for helpful discussions and ATK for the use of ATK 2.0. This paper is in honor of the 60th birthday of George Schatz:

scientist, scholar, friend, colleague, coauthor, and teacher—il miglior fabbro.

References and Notes

(1) Nitzan, A.; Ratner, M. A. *Science* **2003**, *300*, 1384.
(2) Galperin, M.; Ratner, M. A.; Nitzan, A.; Troisi, A. *Science* **2008**, *319*, 1056.
(3) Woitellier, S.; Launay, J. P.; Joachim, C. *Chem. Phys.* **1989**, *131*, 481.
(4) Samanta, M. P.; Tian, W.; Datta, S.; Henderson, J. I.; Kubiak, C. P. *Phys. Rev. B* **1996**, *53*, R7626.
(5) Pauly, F.; Viljas, J. K.; Cuevas, J. C.; Schon, G. *Phys. Rev. B* **2008**, 77.
(6) Finch, C. M.; Sirichantaropass, S.; Bailey, S. W.; Grace, I. M.; Garcia-Suarez, V. M.; Lambert, C. J. *J. Phys.: Condens. Matter* **2008**, 20.
(7) Venkataraman, L.; Klare, J. E.; Nuckolls, C.; Hybertsen, M. S.; Steigerwald, M. L. *Nature* **2006**, *442*, 904.
(8) Donhauser, Z. J.; Mantooth, B. A.; Kelly, K. F.; Bumm, L. A.; Monnell, J. D.; Stapleton, J. J.; Price, D. W.; et al. *Science* **2001**, *292*, 2303.
(9) Mujica, V.; Nitzan, A.; Mao, Y.; Davis, W.; Kemp, M.; Roitberg, A.; Ratner, M. A. In *Electron Transfer: From Isolated Molecules to Biomolecules*; Jortner, J., Bixon, M., Eds.; John Wiley & Sons: New York, 1999; Vol. 107, p 403.
(10) Tsuji, H.; Terada, M.; Toshimitsu, A.; Tamao, K. *J. Am. Chem. Soc.* **2003**, *125*, 7486.
(11) Miller, R. D.; Michl, J. *Chem. Rev.* **1989**, *89*, 1359.
(12) Tamao, K.; Tsuji, H.; Terada, M.; Asahara, M.; Yamaguchi, S.; Toshimitsu, A. *Angew. Chem., Int. Ed.* **2000**, *39*, 3287.
(13) Imhof, R.; Antic, D.; David, D. E.; Michl, J. *J. Phys. Chem. A* **1997**, *101*, 4579.
(14) Albinsson, B.; Teramae, H.; Plitt, H. S.; Goss, L. M.; Schmidbaur, H.; Michl, J. *J. Phys. Chem.* **1996**, *100*, 8681.
(15) Fogarty, H. A.; Tsuji, H.; David, D. E.; Ottosson, C. H.; Ehara, M.; Nakatsuji, H.; Tamao, K.; et al. *J. Phys. Chem. A* **2002**, *106*, 2369.
(16) Plitt, H. S.; Michl, J. *Chem. Phys. Lett.* **1992**, *198*, 400.
(17) Tsuji, H.; Michl, J.; Tamao, K. *J. Organomet. Chem.* **2003**, *685*, 9.
(18) Plitt, H. S.; Downing, J. W.; Raymond, M. K.; Balaji, V.; Michl, J. *J. Chem. Soc., Faraday Trans.* **1994**, *90*, 1653.
(19) Schepers, T.; Michl, J. *J. Phys. Org. Chem.* **2002**, *15*, 490.
(20) Ernst, C. A.; Allred, A. L.; Ratner, M. A. *J. Organomet. Chem.* **1979**, *178*, 119.
(21) Datta, S. *Quantum Transport: Atom to Transistor*; Cambridge University Press: New York, 2005.
(22) Fagas, G.; Greer, J. C. *Nanotechnology* **2007**, *18*, 424010.
(23) Venkataraman, L.; Klare, J. E.; Tam, I. W.; Nuckolls, C.; Hybertsen, M. S.; Steigerwald, M. L. *Nano Lett.* **2006**, *6*, 458.
(24) McDermott, S.; George, C. B.; Fagas, G.; Greer, J. C.; Ratner, M. A. *J. Phys. Chem. C* **2009**, *113*, 744.
(25) Shao, Y.; Molnar, L. F.; Jung, Y.; Kussmann, J.; Ochsenfeld, C.; Brown, S. T.; Gilbert, A. T. B.; et al. *Phys. Chem. Chem. Phys.* **2006**, *8*, 3172.
(26) Becke, A. D. *J. Chem. Phys.* **1993**, *98*, 5648.
(27) Stephens, P. J.; Devlin, F. J.; Chabalowski, C. F.; Frisch, M. J. *J. Phys. Chem.* **1994**, *98*, 11623.
(28) Hay, P. J.; Wadt, W. R. *J. Chem. Phys.* **1985**, *82*, 299.
(29) Brandbyge, M.; Mozos, J. L.; Ordejon, P.; Taylor, J.; Stokbro, K. *Phys. Rev. B* **2002**, *65*, 165401.
(30) Perdew, J. P.; Zunger, A. *Phys. Rev. B* **1981**, *23*, 5048.
(31) Nitzan, A. *J. Phys. Chem. A* **2001**, *105*, 2677.
(32) Tian, W. D.; Datta, S.; Hong, S. H.; Reifenberger, R.; Henderson, J. I.; Kubiak, C. P. *J. Chem. Phys.* **1998**, *109*, 2874.
(33) Evers, F.; Weigend, F.; Koentopp, M. *Phys. Rev. B* **2004**, *69*, 235411.
(34) Ke, S. H.; Baranger, H. U.; Yang, W. T. *J. Chem. Phys.* **2007**, *126*, 201102.
(35) Koentopp, M.; Burke, K.; Evers, F. *Phys. Rev. B* **2006**, *73*, 121403.
(36) Koentopp, M.; Chang, C.; Burke, K.; Car, R. *J. Phys.: Condens. Matter* **2008**, *20*, 083203.
(37) Neaton, J. B.; Hybertsen, M. S.; Louie, S. G. *Phys. Rev. Lett.* **2006**, *97*, 216405.
(38) Reimers, J. R.; Cai, Z. L.; Bilic, A.; Hush, N. S. *Ann. N.Y. Acad. Sci.* **2003**, *1006*, 235.
(39) Thygesen, K. S. *Phys. Rev. Lett.* **2008**, *100*, 166804.
(40) Toher, C.; Filippetti, A.; Sanvito, S.; Burke, K. *Phys. Rev. Lett.* **2005**, *95*, 146402.
(41) Toher, C.; Sanvito, S. *Phys. Rev. Lett.* **2007**, *99*, 056801.
(42) Toher, C.; Sanvito, S. *Phys. Rev. B* **2008**, *77*, 155402.
(43) Hansen, W. N.; Johnson, K. B. *Surf. Sci.* **1994**, *316*, 373.
(44) Sandorfy, C. *Can. J. Chem.* **1955**, *33*, 1337.
(45) Crljen, Z.; Grigoriev, A.; Wendin, G.; Stokbro, K. *Phys. Rev. B* **2005**, *71*, 165316.
(46) Fogarty, H. A.; Casher, D. L.; Imhof, R.; Schepers, T.; Rooklin, D. W.; Michl, J. *Pure Appl. Chem.* **2003**, *75*, 999.
(47) Harrah, L. A.; Zeigler, J. M. *Macromolecules* **1987**, *20*, 601.
(48) Hybertsen, M. S.; Venkataraman, L.; Klare, J. E.; Whalley, A. C.; Steigerwald, M. L.; Nuckolls, C. *J. Phys.: Condens. Matter* **2008**, 20.
(49) Shibano, Y.; Sasaki, M.; Tsuji, H.; Araki, Y.; Ito, O.; Tamao, K. *J. Organomet. Chem.* **2007**, *692*, 356.

JP809963R